Biosensors and Bioelectronics 143 (2019) 111614

Contents lists available at ScienceDirect

Biosensors and Bioelectronics

journal homepage: www.elsevier.com/locate/bios

A novel photoelectrochemical strategy based on an integrative photoactive heterojunction nanomaterial and a redox cycling amplification system for ultrasensitive determination of microRNA in cells

Weijing Yi, Ruili Cai, Dongfang Xiang, Yanxia Wang, Mengsi Zhang, Qinghua Ma, Youhong Cui*, Xiuwu Bian**

Institute of Pathology and Southwest Cancer Center, Key Laboratory of the Ministry of Education, Southwest Hospital, Army Medical University (Third Military Medical University), Chongqing, 400038, China

ARTICLE INFO

Keywords:
Integrative heterojunction nanomaterial
Photoelectrochemical sensor
microRNA
Redox cycling amplification
Ultrasensitive bioassay

ABSTRACT

An ultrasensitive photoelectrochemical (PEC) bioassay for determination of microRNA was proposed based on an integrative photoactive heterojunction nanomaterial to provide the basis of excellent PEC responses and an efficient redox cycling amplification system to improve the detection performances. To establish the bioassay system, the biosensor was firstly modified with Bi_2WO_6@Bi_2S_3 and alkaline phosphatase (ALP). The detection solution was composed of ascorbic acid phosphate (AAP) and ferrocenecarboxylic acid (FcA), where ALP converted AAP into ascorbic acid (AA) to trigger a process of redox cycling amplification by reducing FcA^+ to FcA, resulting in enhanced photocurrent responses of Bi_2WO_6@Bi_2S_3. In the presence of microRNA 21, it could trigger a hybridization chain reaction *via* the special designed hairpin DNA to produce a long repeated DNA sequences to inhibit ALP activity. Thus the reduced ALP activity and consequently decreased photocurrent signal could be obtained for detection of microRNA 21. As expected, this bioassay system performed the satisfactory performances for the ultrasensitive detection of microRNA 21 in the range from 1 fM to 1 nM with an experimental detection limit of 0.26 fM and acceptable practical applicability. Collectively, an efficient PEC bioassay for microRNA 21 is established and this strategy can be expanded to detect other microRNAs, even other molecules in cells.

1. Introduction

MicroRNAs comprise a class of single-stranded noncoding RNAs with 20–30 nucleotides, which are transcribed from the genome and regulate the expression of at least one-third of all human genes (Croce, 2009; Sierzega et al., 2017). In recent years, microRNAs have been utilized as minimally invasive biomarkers to signify the presence of diseases and predict their course, such as cancer, diabetes and cardiovascular diseases (Bam et al., 2018; Rupaimoole and Slack, 2017; Rupaimoole et al., 2016; Thome et al., 2016). Several methods have been established for microRNA analysis. Among them, the quantitative real time polymerase chain reaction (qRT-PCR) as the commercial microRNA analysis technology has been employed as the standard method with high specificity and sensitivity due to its excellent performance of amplification efficiency of polymerase chain reaction (Wu et al., 2017). Other technologies, such as the northbloting and microarray, have also been used for microRNA analysis with high-throughput and low cost (Choi et al., 2017; Schwarzkopf and Pierce, 2016; Zhao et al., 2015). However, the highly homologous sequences, the low concentrations and wide dynamic range of microRNAs result in some limitations for these methods. For example, qRT-PCR method is limited with the imperfect reproducibility and interplatform discrepancies related with the specially designed primer and error-prone enzymatic amplification, whereas northbloting and microarray methods are limited with the inadequate sensitivity and selectivity. Therefore, it is urgent to develop more selective, sensitive and efficient strategies for measurement of microRNAs.

Recently, the photoelectrochemical (PEC) assay as a novel analytical technique has gained considerable attentions due to its desirable advantages, such as low background signal, highsensitivity and cost-effectiveness, and has been successfully employed in some clinical applications (Guo et al., 2019; Kong et al., 2019; Shu et al., 2018; Zhao

* Corresponding author.
** Corresponding author.
E-mail addresses: cuiyouhongx@yahoo.com (Y. Cui), bianxiuwu@263.net (X. Bian).

https://doi.org/10.1016/j.bios.2019.111614
Received 5 July 2019; Received in revised form 5 August 2019; Accepted 19 August 2019
Available online 22 August 2019
0956-5663/

et al., 2014). In the PEC platform, the additional light energy was employed as the input source to generate photocurrent for PEC assay with extremely low background signal. Furthermore, the PEC responses could be enhanced easily *via* sensitizer with high photocurrent conversion efficiency, such as CdS, PbS, C_3N_4 and Bi_2S_3 with stable chemical properties, unique PEC properties and convenient modification (Huang et al., 2018; Li et al., 2017; Wang et al., 2015, 2017; Ye et al., 2016; Zhao et al., 2018a,b). With the rapid development of nanotechnologies, various new PEC indicators and sensitizers named as heterojunction PEC materials were proposed to improve the photocurrent conversion efficiency for sensitive detection of biomarkers in clinical samples. Very recently, Zhao's group reported the Bi_2WO_6/Bi_2S_3 heterojunction PEC strategy, which generated significantly enhanced PEC responses and was employed for the ultrasensitive detection of myoglobin for clinical diagnosis (Wang et al., 2018). In these composite heterojunction PEC materials, the contact area between PEC indicator and sensitizer has improved by enhancing the surface area of indicator and sensitizer, but the improvement was still limited, especially on the photocurrent conversion efficiency and PEC performances. On the other hand, some reducing (or oxidizing) agents were essential as the PEC reaction substrates in the detection solution to help the PEC indicator to generate the PEC current, while they were consumed with the PEC reaction, and thus limited the stability and sensitivity of the related PEC strategies. Notably, the reducing (or oxidizing) agents could be regenerated based on the repeatedly coupled reduction and oxidation reaction, named as the redox cycling amplification, in the electrochemical detections, which may be helpful to improve the PEC performances, especially the detection sensitivity (Cao et al., 2018; Haque et al., 2015; Park et al., 2014). Considering the challenges and promising advantages, therefore, an ultrasensitive PEC strategy could be expected based on the integrative heterojunction PEC material and efficient redox cycling amplification system.

Herein, we proposed an ultrasensitive PEC strategy based on the integrative photoactive heterojunction nanomaterial providing the basis of excellent PEC responses and the efficient redox cycling amplification system to improve the detection performances of PEC bioanalysis. Briefly, as shown in Scheme 1, the $Bi_2WO_6@Bi_2S_3$ integrative composite nanomaterial was modified onto the glass carbon electrode (GCE) surface to generate a basic PEC signal, which was employed to immobilize alkaline phosphatase (ALP) on the electrode surface also. At the same time, the redox cycling amplification system was performed consisting of the redox mediator and signaling indicator produced from ALP assisted enzymatic reaction, in which the ferrocenecarboxylic acid (FcA) was employed as the redox mediator by the holes in the $Bi_2WO_6@Bi_2S_3$ integrative composite nanomaterial to trigger the redox cycling amplification process *via* the oxidization of FcA to FcA^+, and ascorbic acid (AA) sourced from the ALP-based enzymatic conversion of ascorbic acid phosphate (AAP) was employed as the signaling indicator. And thus, a significantly amplified PEC signal could be obtained. In the presence of microRNA 21, it could open the self-designed special hairpin structure of hairpin 1, triggering a similar hybridization chain reaction with exposure of a new terminus, in turn, to open the hairpin structure of hairpin 2, hairpin 3 and hairpin 4, respectively. Based on the special hybridization chain reaction, a long repeated DNA sequences with large amounts of efficient DNA inhibitor to ALP could be obtained, which were employed to react with the ALP immobilized on the electrode surface to generate a decreased PEC signal due the reduced ALP-based enzymatic conversion of AAP to AA *via* inhibited enzymatic activity of ALP. Thus, the expression of microRNA 21 would be calculated based on the decreased PEC signal. Importantly, the detection sensitivity was improved significantly *via* the integrative heterojunction PEC materials, efficient redox cycling amplification system and efficient generation of ALP inhibitor *via* the special hybridization chain reaction. The proposed PEC strategy could be easily expanded for the ultrasensitive detection of various other microRNAs, providing a new avenue for early clinical diagnosis.

2. Experimental methods

2.1. Reagents and materials

Sodium tungstate ($Na_2WO_4{\cdot}2H_2O$), bismuth nitrate ($Bi(NO_3)_3{\cdot}5H_2O$), sodium sulfide ($Na_2S{\cdot}9H_2O$), ethanediol, AAP and FcA was purchased from Sigma Chemical Co. (MO, USA). Dulbecco's modified eagle's medium (DMEM), fetal bovine serum, penicillin and streptomycin were purchased from Gibco Laboratories Life Technologies Inc. (NY, USA). Trizol reagent was obtained from TIANGEN Biotech Co., Ltd. (Beijing, China). Tris-buffer with ethylenediaminetetraacetic acid (TE) and phosphate buffer saline (PBS) buffer were purchased from Beyotime Institute of Biotechnology (Jiangshu, China). Ultrapure water (18.2 MΩ/cm) was used throughout this work.

All of the oligonucleotides employed in this work (Table S1) were

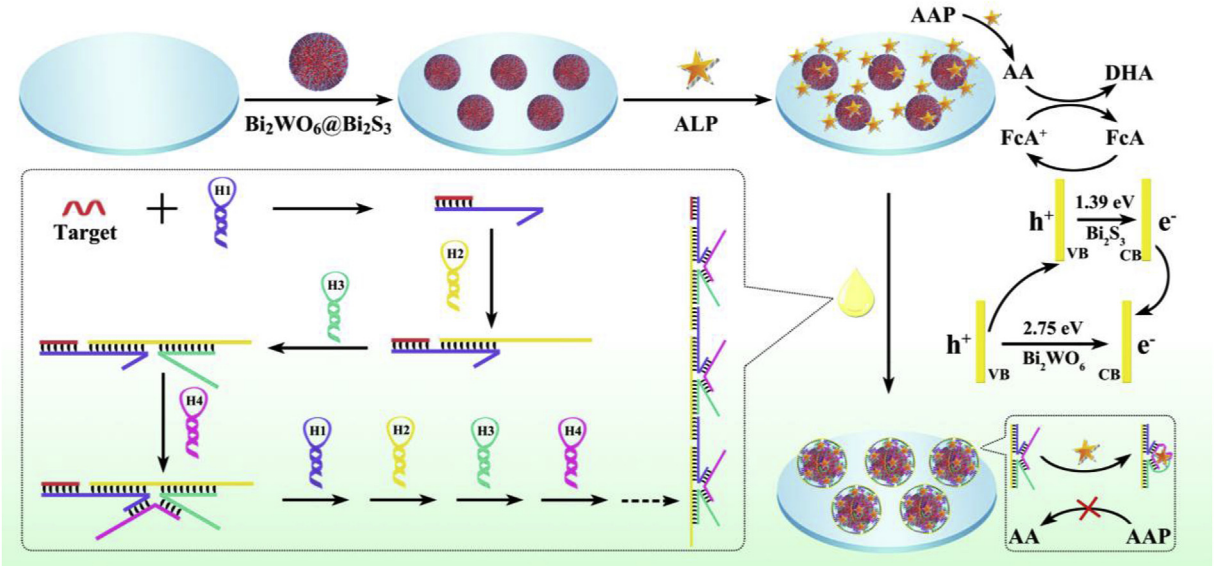

Scheme 1. Schematic diagrams of the proposed PEC assay *via* integrative photoactive $Bi_2WO_6@Bi_2S_3$ heterojunction nanomaterial and the efficient redox cycling amplification system.

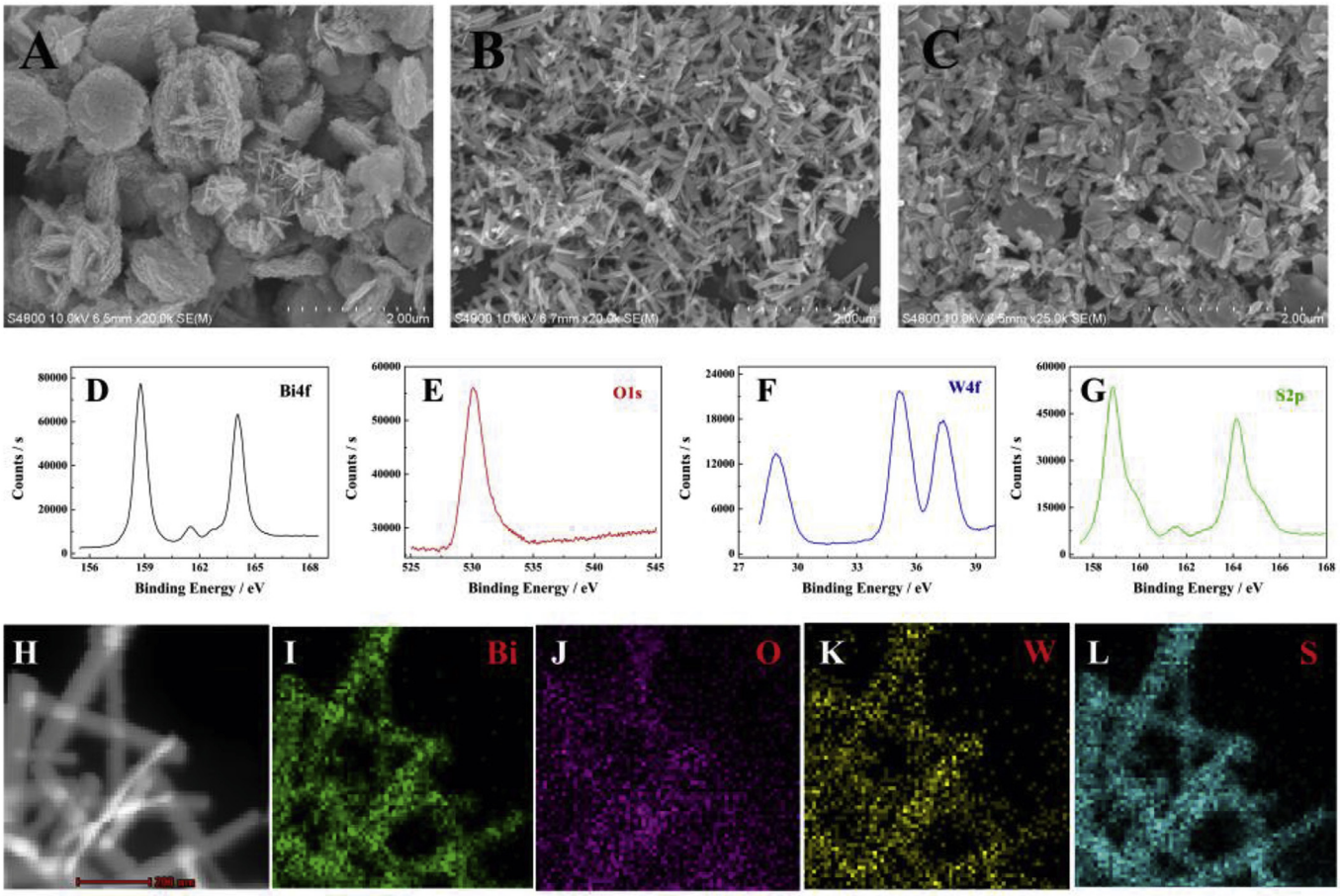

Fig. 1. A-C, Morphology characterizations for Bi_2WO_6 nanomaterials (A) and Bi_2S_3 nanomaterial (B) and Bi_2WO_6@Bi_2S_3 heterojunction nanomaterial by SEM. D-G, XPS characterizations for Bi_2WO_6@Bi_2S_3 heterojunction nanomaterial with Bi4f (D), O1s (E), W4f (F) and S2p (G), respectively; H-L, elemental mapping characterizations for the Bi_2WO_6@Bi_2S_3 nanomaterial with the elements of Bi (I), O (J), W (K) and S (L), respectively.

synthesized by Shanghai Sangon Biological Engineering Technology and Services Co., Ltd. (Shanghai, China), in which all hairpin oligonucleotides were firstly heated to 95 °C for 2 min and cooled to room temperature to form stem-loop structure.

2.2. Apparatus

Electrochemical measurements, including cyclic voltammetry (CV) and electrochemical impedance spectroscopy (EIS), were carried out on CHI 660e electrochemical workstation (CH Instruments Inc., Shanghai, China). All of the PEC measurements were performed on PEC workstation (Ivium, Netherlands). All of the electrochemical and PEC measurements were carried out with a conventional three-electrode system with a platinum wire as auxiliary electrode, an Ag/AgCl as reference electrode and a glassy carbon electrode (GCE) with or without modification as the working electrode, respectively. UV–*vis* absorption spectroscopy was carried out on a UV-2450 UV–*vis* spectrophotometer (Shimadzu, Tokyo, Japan). The X-ray photoelectron spectrum (XPS) was performed on a VG Scientific ESCALAB 250 spectrometer (Thermoelectricity Ins., USA). The morphologies of the nanomaterial were characterized with a scanning electron microscopy (SEM, S-4800, Hitachi, Japan) and transmission electron microscopy (TEM, JEM-2100, JEOL, Japan). The fluorescent microscopy was performed on a laser confocal microscope (Leica Onc., Heidelbery, Germany).

2.3. Cell culture

In this work, cervical cancer Hela cells and human breast cancer MCF-7 cells were employed as the detection model for the potential application study of the proposed PEC bioassay, which were purchased from the Type Culture Collection of the Chinese Academy of Sciences (Shanghai, China). All of the cells were grown in DMEM medium with 10% foetal bovine serum, 100 U/mL penicillin and 100 U/mL streptomycin, and maintained in a humidified atmosphere with 5% CO_2 at 37 °C. The microRNA were extracted from the cultured cells according to the manufacturer protocol after cell counting.

2.4. Fabrication of the PEC biosensor for microRNA assay

Firstly, all of the GCE (diameter = 4 mm) was polished with alumina slurries (0.3 and 0.05 μm, respectively) carefully and ultrasonicated in deionized water and ethanol to remove the physically adsorbed materials. Then, the prepared Bi_2WO_6@Bi_2S_3 heterojunction nanomaterial was dropped onto the electrode surface and dried in air. Subsequently, the modified electrode was incubated with ALP at 4 °C to immobilize ALP on the modified electrode. After each step, the electrode was washed with distilled water to remove the unbounded reagents. Furthermore, the fabrication of the PEC biosensor was characterized by CV and EIS in 5 mM $[Fe(CN)_6]^{3-/4-}$ solution.

2.5. PEC measurement procedure

The PEC measurements were performed in the detection solution of 5 mL PBS (0.1 M, pH 7.0) solution with or without AAP and FcA. In our experiments, the excitation light sources were provided by the LED lamp and the excitation light was switched off-on-off for 10 s-20 s–10 s

under 0.0 V potential. For the detection of experimental or real samples, 5 μL of sample was added into the TE buffer with hairpin DNA (20 μL), and the mixture was hold at 37 °C for target trigger DNA hybridization. Subsequently, 10 μL of the mixture was added onto the electrode for the reaction between DNA inhibitors and ALP at 37 °C for 1 h. After washing with distilled water, the reacted electrode was employed for the PEC measurements.

3. Results and discussion

3.1. Characterizations of the synthesized nanomaterial

In this work, the integrative photoactive Bi_2WO_6@Bi_2S_3 heterojunction nanomaterial was characterized based on the SEM firstly with Bi_2WO_6 and Bi_2S_3 as controls. The Bi_2WO_6 nanomaterial performed nanosheet-assembled microdisc structure and the Bi_2S_3 showed a nanorod structure as can be seen in the SEM images (Fig. 1). For the prepared Bi_2WO_6@Bi_2S_3 heterojunction nanomaterial, some nanorod and microdisc-like structure could been seen, indicating the composition between Bi_2WO_6 and Bi_2S_3 nanomaterial. Further characterizations based on the XPS for the elemental analysis of the proposed Bi_2WO_6@Bi_2S_3 heterojunction nanomaterial, it performed all of the characteristic peaks for Bi4f (158.75 and 164.05 eV), O1s (530.10 eV), W4f (29.05 and 35.15 and 37.35 eV), and S2p (158.85 and 164.15 eV), which confirmed the coexisting of the Bi_2WO_6 and Bi_2S_3 nanomaterial. Additionally, EDS mapping was employed for the elemental distribution of the Bi_2WO_6@Bi_2S_3 heterojunction nanomaterial. As expected, the elemental distribution images of Bi, W, O and S were well-distributed and overlaid well with the image of the Bi_2WO_6@Bi_2S_3 heterojunction nanomaterial, suggesting the Bi_2WO_6 and Bi_2S_3 nanomaterial was integrative, which was helpful to transfer electrons among them, providing the great potentials for highly efficient PEC reactions.

3.2. Characterizations of the PEC biosensor based on electrochemical measurements

In this experiment, the fabrication procedures of the PEC biosensor were characterized by electrochemical measurements step by step as shown in Fig. 2. The stepwise fabrication of the PEC biosensor was firstly characterized based on CV measurements at different stages with redox probe of $[Fe(CN)_6]^{3-/4-}$ in a potential range from −0.3 to 0.7 V (Fig. 2A). A well-defined redox peaks the $[Fe(CN)_6]^{3-/4-}$ was obtained for the bare GCE (curve a), indicating the well preparation of the clean GCE. After the modification of Bi_2WO_6@Bi_2S_3 heterojunction nanomaterial on the electrode surface, the redox peak current decreased with an increased oxidation-reduction potential. When the ALP was immobilized on the Bi_2WO_6@Bi_2S_3 modified electrode surface *via* the excellent adsorption function of Bi_2WO_6@Bi_2S_3 with large surface area, the redox peak current decreased significantly due to the resistance effect of ALP, suggesting the successful immobilization of ALP on the electrode surface. In addition, another important electrochemical technology, EIS, was employed to characterize the fabrication of the proposed PEC biosensor in 5 mM $[Fe(CN)_6]^{3-/4-}$ in a frequency range from 5×10^{-2} to 1×10^{6} Hz (Fig. 2B), in which the electron transfer resistance (R_{et}) as an important factor of EIS to demonstrate the electron transfer kinetics on the electrode interface was employed to characterize the electrode modification quantitatively. For the bare GCE, there was a small semicircle with R_{et} of about 50 Ω. When the Bi_2WO_6@Bi_2S_3 heterojunction nanomaterial was modified onto the electrode surface, the resistance increased largely to about 600 Ω. After the immobilization of ALP onto the Bi_2WO_6@Bi_2S_3 modified electrode surface, the resistance increased remarkably to about 1800 Ω because the ALP with non-electroactive property impeded the electron transfer. All of the CV and EIS characterizations confirmed the successful fabrication of the PEC biosensor as expected.

3.3. Comparison of different photoactive nanomaterial and PEC biosensor

In order to investigate the photochemical efficiency of the proposed PEC strategy based on the integrative photoactive heterojunction nanomaterial (Bi_2WO_6@Bi_2S_3 heterojunction nanomaterial) and the efficient redox cycling amplification system (ALP-AAP-FcA), various comparison studies were conducted to contrast the photocurrent responses of different photoactive heterojunction nanomaterial, including Bi_2WO_6, Bi_2S_3, Bi_2WO_6/Bi_2S_3 and Bi_2WO_6@Bi_2S_3 heterojunction nanomaterial, and PEC biosensors with or without special redox cycling amplification reagent, including ALP, AAP and FcA. As shown in Fig. 3A, these were small photocurrent responses for the Bi_2WO_6 and Bi_2S_3 modified electrode, specially 9.0 μA and 0.8 μA, respectively. For the Bi_2WO_6/Bi_2S_3 heterojunction nanomaterial, an enhanced photocurrent signal was obtained due to the good molecular level matching between Bi_2WO_6 and Bi_2S_3 nanomaterial. About 18.5 μA photocurrent response was achieved for the Bi_2WO_6@Bi_2S_3 heterojunction nanomaterial modified electrode, which was significantly higher than that of Bi_2WO_6, Bi_2S_3 and Bi_2WO_6/Bi_2S_3 nanomaterial due to the good band matching and increased surface contact between Bi_2WO_6 and Bi_2S_3 nanomaterial. Briefly, the enhancement of photocurrent response could be explained as shown in Scheme 1. The electron-hole pairs could be generated initially by the light illumination within both Bi_2WO_6 and Bi_2S_3 nanomaterial. The electrons on the conduction band (CB) of Bi_2S_3 were transferred to the CB of Bi_2WO_6 and then collected by GCE to perform as the photocurrent signal. At the same time, the holes on the valence band (VB) of Bi_2WO_6 injected to the VB of Bi_2S_3 rapidly. Compared with Bi_2WO_6 and Bi_2S_3 nanomaterial, the Bi_2WO_6@Bi_2S_3 and Bi_2WO_6/Bi_2S_3 heterojunction nanomaterial accelerated the transfer of photo-excited charge carriers with significantly enhanced photocurrent response, and the formation of the Bi_2WO_6@Bi_2S_3 heterojunction nanomaterial generated the increased surface contact between Bi_2WO_6 and Bi_2S_3 nanomaterial and thus enhanced the photocurrent response furtherly.

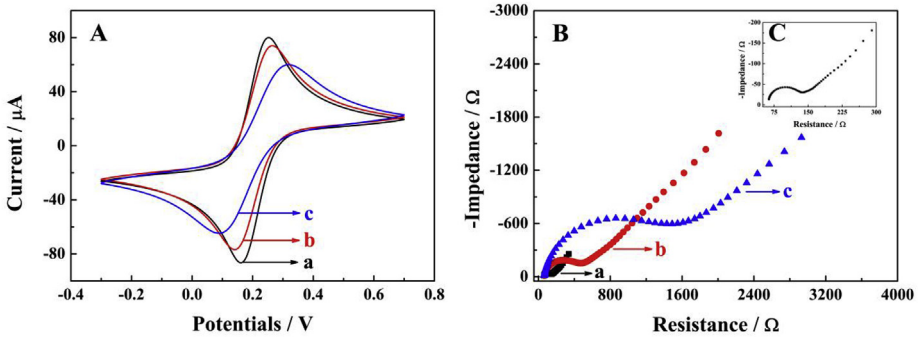

Fig. 2. Characterizations for the stepwise fabrication of the proposed PEC biosensors based on CV (A) and EIS (B), curve a, bare GCE; curve b, Bi_2WO_6@Bi_2S_3 modified GCE electrode; curve c, Bi_2WO_6@Bi_2S_3 modified GCE electrode after the immobilization of ALP. Inset of Fig. 2B, the EIS result of bare GCE.

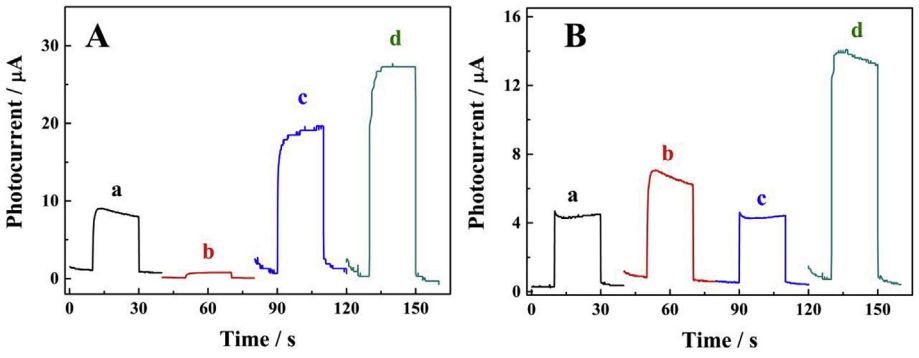

Fig. 3. A, PEC responses of Bi_2WO_6 (curve a), Bi_2S_3 (curve b), Bi_2WO_6/Bi_2S_3 (curve c) and Bi_2WO_6@Bi_2S_3 (curve d) heterojunction nanomaterial; B, PEC tests of Bi_2WO_6@Bi_2S_3 nanomateials with or without special redox cycling amplification reagents including (a) Bi_2WO_6@Bi_2S_3 modified electrode with AAP and FcA in the detection solution; (b) ALP/Bi_2WO_6@Bi_2S_3 modified on the electrode surface with AAP in the detection solution; (c) ALP/Bi_2WO_6@Bi_2S_3 modified on the electrode surface with FcA in the detection solution; and (d) ALP/Bi_2WO_6@Bi_2S_3 modified on the electrode surface with AAP and FcA in the detection solution, respectively.

For the comparison of different PEC biosensor with or without special redox cycling amplification reagent, four kinds of PEC biosensors including (A) Bi_2WO_6@Bi_2S_3 modified electrode with AAP and FcA in the detection solution; (B) ALP/Bi_2WO_6@Bi_2S_3 modified electrode with AAP in the detection solution; (C) ALP/Bi_2WO_6@Bi_2S_3 modified electrode with FcA in the detection solution; and (D) ALP/Bi_2WO_6@Bi_2S_3 modified electrode with AAP and FcA in the detection solution. As can be seen in Fig. 3B, without the enzymatic dephosphorylation of ALP on AAP to generate AA (curve a), there was an enhanced photocurrent signal just attributed to the oxidization of FcA by light generating holes and the subsequent electron-hole pair recombination on Bi_2WO_6@Bi_2S_3 nanomaterial. For the ALP/Bi_2WO_6@Bi_2S_3 modified electrode with AAP in the detection solution, the AAP could be changed to AA by the enzymatic dephosphorylation of ALP, which could enhance the photocurrent performances obviously (curve b). For the ALP/Bi_2WO_6@Bi_2S_3 modified electrode with FcA in the detection solution (curve c), a photocurrent response similar with curve a was achieved due to the similar enhancement functions of FcA. In the presence of both AAP and FcA in the detection solution for the ALP/Bi_2WO_6@Bi_2S_3 modified electrode (curve d), an obviously enhanced photocurrent signal was obtained, which performed the largest enhancement in these comparison systems, indicating the highly efficient amplification effect of the proposed redox cycling amplification *via* ALP-AAP-FcA on the Bi_2WO_6@Bi_2S_3 heterojunction nanomaterial, which is important and necessary for the ultrasensitive bioassay.

3.4. Photoelectrochemical characterizations of the prepared biosensor

The PEC characterizations for the fabrication of the proposed biosensor were performed based on the photocurrent responses step by step in the detection solution with AAP and FcA as the redox cycling amplification reagents. As shown in Fig. S5A, there was no obvious photocurrent response for the bare GCE electrode (curve a). After the modification of the Bi_2WO_6@Bi_2S_3 heterojunction nanomaterial (curve b), there was an obvious photocurrent signal of 42.8 μA based on the enhancement effect of FcA on the Bi_2WO_6@Bi_2S_3 heterojunction nanomaterial. When the ALP was immobilized on the electrode surface (curve c), it performed a significantly enhanced photocurrent signal due to the highly efficient redox cycling amplification based on the ALP-AAP-FcA on the Bi_2WO_6@Bi_2S_3 heterojunction nanomaterial. In the presence of target microRNA 21 (Fig. S5B), it could trigger the special hybridization chain reaction to generate amounts of inhibitors for ALP to inhibit the enzymatic generation of AA from AAP, performing a significantly decreased photocurrent signal, which indicated the potential for sensitive detection of microRNA 21.

3.5. Application of the proposed PEC bioassay

The application performances of the proposed PEC bioassay was studied under the optimal conditions with variable concentrations of target microRNA 21 in the range from 1 fM to 1 nM. As shown in the Fig. 4A, the photocurrent responses were decreased along with the increased concentration of microRNA 21, which could be attributed to more microRNA 21 causing the enhanced generation of inhibitor for ALP to decrease the generation of AA and thus to inhibite the regeneration of FcA, performing decreased photocurrent signals related with the concentration of microRNA 21. Additionally, as can be seen in the Fig. 4B with the corresponding linear curve, the relationship between the photocurrent signal of the proposed PEC bioassay and the concentration of microRNA 21 could be described in the equation $I = -1.67c_{\text{microRNA 21}} + 3.61$ (I was the photocurrent response of the proposed PEC bioassay and the $c_{\text{microRNA 21}}$ was the concentration of the microRNA 21) within the range from 1 fM to 1 nM with an experimental detection limit of 0.26 fM, which was comparable to that in some recent references (Table S2).[23-27]

In addition, the selectivity as one of the important properties of the PEC bioassay was studied by using the interfering microRNAs, such as the microRNA 141, microRNA 122, microRNA 155, let 7a, and their mixture plus the target. As shown in Fig. S6A, the target microRNA 21 and the mixture sample performed smaller photocurrent signals than that of these interferences, and the results of these interferences were similar to that of the black sample, which indicated the acceptable selectivity of the proposed PEC bioassay for detection of microRNA 21. Furthermore, the stability as one of the other important properties of the PEC bioassay was evaluated based on the repeated measurements within 10 cycles and long-time tests within 30 days. There was no significant changes in the photocurrent responses in these studies, indicating the good stability of the proposed PEC bioassay for the sensitive detection of microRNA 21.

The practical applicability of the proposed PEC bioassay was evaluated based on the analysis of real samples from different cell lines, such as the human breast cancer MCF-7 cells and cervical cancer Hela cells. As shown in Fig. S6B with the photocurrent responses of the proposed PEC bioassay for these cell lines with different concentrations, the photocurrent signals decreased with the cell numbers and the photocurrent signals of MCF-7 cells with high expression of microRNA 21 were lower than that of Hela cells with low expression of microRNA 21, which was confirmed with some previous reports, suggesting the potential application of the proposed PEC bioassay for clinical real samples. Furthermore, the recovery tests of the proposed PEC bioassay for target microRNA 21 was measured by the standard addition method in clinical real serums, which performed acceptable results in the range of 93.0–104.2% with RSD of less than 5.3%. All of these application studies indicated the acceptable accuracy for the sensitive detection of microRNA 21 in real samples.

4. Conclusion

In summary, an ultrasensitive PEC bioassay was proposed based on the integrative photoactive heterojunction nanomaterial to provide the basis of excellent PEC responses and the efficient redox cycling amplification system to improve the detection performances of PEC

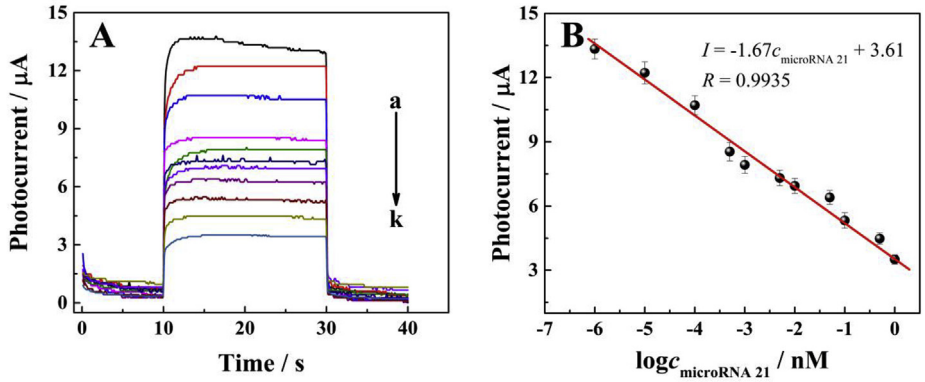

Fig. 4. A. PEC responses of the proposed PEC bioassay to different concentration of microRNA 21 (a, 1 fM; b, 10 fM; c, 100 fM; d, 1 pM; e, 5 pM; f, 10 pM; g, 50 pM; h, 100 pM; i, 500 pM and k, 1 nM); B. the as-derived linear curve for the relationship between the PEC signal and logarithm of concentration of microRNA 21.

bioanalysis. In the presence of target microRNA 21, it could trigger a special hybridization chain reaction to inhibit ALP, resulting in the reduced enzymatic conversion of AAP to AA, and thus to reduce the efficiency of redox cycling amplification system to generate a decreased photocurrent signal associated with the concentration of microRNA 21. This system showed the satisfactory performances for the ultrasensitive detection of microRNA 21 in the range from 1 fM to 1 nM with an experimental detection limit of 0.26 fM and acceptable practical applicability. Importantly, this efficient PEC bioassay system could be expanded to detection of various biomarkers, offering new avenues for early clinical diagnosis.

CRediT authorship contribution statement

Weijing Yi: Conceptualization, Data curation, Formal analysis, Writing - original draft. **Ruili Cai:** Data curation, Formal analysis. **Dongfang Xiang:** Data curation, Validation. **Yanxia Wang:** Data curation, Formal analysis. **Mengsi Zhang:** Data curation, Formal analysis. **Qinghua Ma:** Data curation, Validation. **Youhong Cui:** Conceptualization, Writing - review & editing. **Xiuwu Bian:** Conceptualization, Funding acquisition, Writing - review & editing.

Declaration of competing interest

The authors declare that they have no known competing financial interests or personal relationships that could have appeared to influence the work reported in this paper.

Acknowledgment

This work was supported by grant from National Natural Science Foundation of China (Innovative research group projects, 81821003), General Financial Grant from the China Postdoctoral Science Foundation (2014M562595) and Special Financial Grant from the Chongqing Postdoctoral Science Foundation (Xm2014049).

Appendix A. Supplementary data

Supplementary data to this article can be found online at https://doi.org/10.1016/j.bios.2019.111614.

References

Bam, M., Yang, X., Sen, S., Zumbrun, E.E., Dennis, L., Zhang, J., Nagarkatti, P.S., Nagarkatti, M., 2018. Mol. Neurobiol. 55, 1419–1429.
Cao, J.T., Wang, B., Dong, Y.X., Wang, Q., Ren, S.W., Liu, Y.M., Zhao, W.W., 2018. ACS Sens. 3, 1087–1092.
Choi, Y.S., Edwards, L.O., DiBello, A., Jose, A.M., 2017. Nucleic Acids Res. 45, 87.
Croce, C.M., 2009. Nat. Rev. Genet. 10, 704–714.
Guo, X.X., Liu, S.P., Yang, M.H., Du, H.T., Qu, F.L., 2019. Biosens. Bioelectron. 139, 111312.
Haque, A.M.J., Kim, J., Dutta, G., Kim, S., Yang, H., 2015. Chem. Commun. 51, 14493–14496.
Huang, W., Xing, C., Wang, Y., Li, Z., Wu, L., Ma, D., Dai, X., Xiang, Y., Li, J., Fan, D., Zhang, H., 2018. Nanoscale 10, 2404–2412.
Kong, W.S., Tan, Q.Q., Guo, H.Y., Sun, H., Qin, X., Qu, F.L., 2019. Microchimica Acta 186, 73.
Li, X., Zhu, L., Zhou, Y., Yin, H., Ai, S., 2017. Anal. Chem. 89, 2369–2376.
Park, S., Singh, A., Kim, S., Yang, H., 2014. Anal. Chem. 86, 1560–1566.
Rupaimoole, R., Calin, G.A., Lopez-Berestein, G., Sood, A.K., 2016. Cancer Discov. 6, 235–246.
Rupaimoole, R., Slack, F.J., 2017. MicroRNA therapeutics: towards a new era for the management of cancer and other diseases. Nat. Rev. Drug Discov. 16, 203–222.
Schwarzkopf, M., Pierce, N.A., 2016. Nucleic Acids Res. 44, 503.
Shu, J., Qiu, Z., Lv, S., Zhang, K., Tang, D., 2018. Anal. Chem. 90, 2425–2429.
Sierzega, M., Kaczor, M., Kolodziejczyk, P., Kulig, J., Sanak, M., Richter, P., 2017. J. Cancer 117, 266–273 Br.
Thome, A.D., Harms, A.S., Volpicelli-Daley, L.A., Standaert, D.G.J., 2016. Neuroscience 36, 2383–2390.
Wang, G.L., Shu, J.X., Dong, Y.M., Wu, X.M., Zhao, W.W., Xu, J.J., Chen, H.Y., 2015. Anal. Chem. 87, 2892–2900.
Wang, H., Zhang, Q., Yin, H., Wang, M., Jiang, W., Ai, S., 2017. Biosens. Bioelectron. 95, 124–130.
Wang, B., Mei, L.P., Ma, Y., Xu, Y.T., Ren, S.W., Cao, J.T., 2018. Anal. Chem. 90, 12347–12351.
Wu, H., Wang, J., Ma, H., Xiao, Z., Dong, X., 2017. Oncotarget 8, 92914–92925.
Ye, C., Wang, M.Q., Gao, Z.F., Zhang, Y., Lei, J.L., Luo, H.Q., Li, N.B., 2016. Anal. Chem. 88, 11444–11449.
Zhao, W.W., Xu, J.J., Chen, H.Y., 2014. Chem. Rev. 114, 7421–7441.
Zhao, Y., Chen, F., Li, Q., Wang, L., Fan, C., 2015. Chem. Rev. 115, 12491–12545.
Zhao, W.W., Xu, J.J., Chen, H.Y., 2018a. Anal. Chem. 90, 615–627.
Zhao, Y., Gong, J., Zhang, X.B., Kong, R.M., Qu, F.L., 2018b. Sens. Actuators B Chem. 255, 1753–1761.